ELSEVIER

Journal of Alloys and Compounds 303–304 (2000) 198–206

Journal of ALLOYS AND COMPOUNDS

www.elsevier.com/locate/jallcom

Electron transfer processes in rare earth doped insulators

U. Happek[a,*], S.A. Basun[b], J. Choi[a], J.K. Krebs[a], M. Raukas[c]

[a]*Department of Physics and Astronomy, The University of Georgia, Athens, GA 30602, USA*
[b]*A.F. Ioffe Physico-Technical Institute, St. Petersburg, Russia*
[c]*Osram Sylvania, Inc., Research and Development, Beverly, MA 01915, USA*

Abstract

The optical properties of insulators activated with rare earth ions are determined by the energy levels of the impurity; hence, the study of intra-ion transitions has been the principal focus of numerous investigations in the past. This has occurred to the neglect of other properties, particularly those involving the most energetic states of the impurity. To understand the optical properties in regions of higher energy, i.e. UV, the intrinsic bands of the host materials and the charge transfer dynamics between impurity and host must be taken into account. In such cases, the exact positions of the impurity states relative to the host conduction and valence bands become important and need to be determined in order to establish the physical behavior of the activated material. A complete treatment of the impurity–host system leads to a donor–acceptor model, similar to the common approach in semiconductor physics. Here we apply this model to discuss recent experiments on rare earth doped materials, including the luminescence efficiency of rare earth doped scintillator and phosphor materials, and laser cooling of solids.

Keywords: Photoconductivity; Insulators

1. Introduction

The optical properties of rare earth activated insulators are determined by the energy levels of the impurity, mainly by intra-ion f–f transitions that are weakly perturbed by the host. The wave functions of energetically higher states (d-orbitals) interact more strongly with the host system; nevertheless, it has been customary to consider the impurity electrons independently from the surroundings. The host environment influences the impurity electrons via the crystal field of certain symmetry and strength, leading to the energy splitting and shifting of the free ion orbitals [1]. However, it has become evident in recent years that a thorough understanding of the host–impurity system requires the incorporation of excitation processes that involve both the impurity electronic states and the extended electronic states of the host lattice, i.e. the valence and conduction bands. This approach leads to a donor–acceptor model for the impurity host system, a model that is used extensively for doped semiconductors [2,3]. This newly emerging point of view for describing doped insulators is partly related to the rising activity in scintillator and phosphor research where the application of these materials require excitation energies larger than the bandgap of the host, often leading to electron transfer processes [4]. Spectral holeburning (chemical holeburning) is another field that requires the knowledge of impurity energy levels with respect to the host bands. Spectral holeburning is an important tool to investigate the fundamental dynamical properties of ordered and disordered materials [5]. More recently, holeburning processes are extensively studied for high density data storage. Finally, at the theoretical front, an increasing number of calculations on the energy levels of doped systems are published, and there is a need for experimental data to test the different theoretical techniques. While in a local description of the impurity ion the electron transfer processes can be taken into account as ionization and charge transfer processes, we believe that certain phenomena, like photoconductivity in doped insulating materials, where charge transfer is observed over macroscopic distances, are more

*Corresponding author. Tel.: +1-706-542-2859; fax: +1-706-542-2492.

E-mail address: uhappek@hal.physast.uga.edu (U. Happek)

0925-8388/00/$ – see front matter
PII: S0925-8388(00)00630-7

properly treated in the donor/acceptor model for the impurity–host system.

2. Electron transfer processes and Born–Haber cycle

For a stable impurity ion (M^{n+}) with a ground state located within the host bandgap, two electron transfer processes are possible:

(a) Transfer of a valence band electron to an empty impurity ion level. This process leaves a hole in the host valence band. Since in this process the impurity ion accepts an electron ($M^{n+} \rightarrow M^{(n-1)+}$) it is called an acceptor-like charge transfer process.

(b) Transfer of an electron from a filled impurity state to the conduction band. This process ionizes the impurity ion ($M^{n+} \rightarrow M^{(n+1)+}$) and since the electron is donated to the host conduction band it is called a donor-like charge transfer process or photoionization.

Applying this concept to a trivalent rare earth impurity RE^{3+}, Fig. 1 shows the location of the highest occupied 4f ground state level within the forbidden gap of the host. The host valence and conduction band are separated by E_G. The photon energy for a donor process ($RE^{3+} \rightarrow RE^{4+} + e^-$), i.e. promoting the electron from the highest occupied ground state level to the conduction band is given by $h\nu_D > E_D$, where E_D is the energy difference between the bottom of the conduction band and the rare earth electronic level under consideration. This process leaves the rare earth ion in the tetravalent state. The RE^{4+} ion can be converted back to a RE^{3+} ion in an acceptor like process ($RE^{4+} \rightarrow RE^{3+} + e^+$) by transferring an electron from the valence band to the 4f shell of the RE^{4+} ion, thus converting RE^{4+} to RE^{3+}. As a result, this electron will occupy the highest filled f-level of the RE^{3+} ground state configuration, leaving a hole (e^+) in the valence band. Thus the photon energy for an acceptor process is given by $h\nu_A > E_A$, where E_A is the energy difference between the highest occupied 4f ground-state level of the RE^{3+} ion and the top of the valence band. It becomes evident from Fig. 1 that E_A, E_D, and E_G are related through

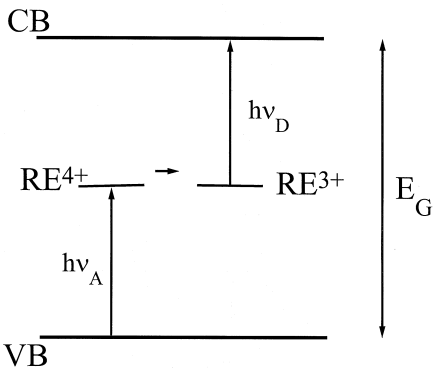

Fig. 1. Acceptor- and donor-like electron transfer processes in doped insulators.

$$E_G = E_A + E_D,$$

which states that the energies for the donor and acceptor like electron transfer processes add up to the value of the band gap of the host material. This relation is valid for zero phonon transitions at $T = 0$ K, thus, direct comparison with experimental data is not always straight forward. The relation between acceptor, donor and band gap energies can be derived using the Born–Haber cycle, which originally described a method of estimating the cohesive energy of ionic lattices [6,7]. It is based on thermodynamic principles only, with no specific impurity or host features involved, which makes it very general and applicable to any impurity in any host. The Born–Haber cycle was further developed by McClure and coworkers to find the relationship between photoionization and charge transfer processes of impurity ions [2]. Adopting the band model for impurity ions in insulators, it becomes evident that ionic states involving unoccupied levels resonant with the valence band or occupied levels resonant with the conduction band are unstable.

3. Photoconductivity experiments on doped insulators

Several techniques can be employed to locate the energy level of impurity ions with respect to the host valence and conduction bands. X-ray photoelectron spectroscopy (XPS) measures directly the electron density as a function of binding energy, providing, in principle, the energy levels of both host and impurity ions [8]. However, in practice the energy levels for impurity ions can often be measured only for relatively high concentrations. Optical absorption measurements as a function of frequency will also provide the energy level of impurities relative to the host bands, since both acceptor- and donor-like processes require the absorption of photons. As will be shown later, intra-ion transitions, especially broad f–d transitions can be superimposed on the absorption due to electron transfer processes, making the interpretation ambiguous. The experimental technique of choice to study delocalized transitions in doped insulators is photoconductivity [9,10], a method that allows one to determine the position of impurity energy levels with respect to the host bands even for low impurity concentrations (less than 0.1 mol%). Conventionally, this technique is used in semiconductor physics, but a similar, although refined, approach can be applied to insulators as well. McClure and coworkers have used this technique to determined the positions of impurity energy levels in the host lattice bandgap in a variety of systems [2, 11, 12]. Photoconductivity is a powerful method that provides extremely useful information especially for non-luminescent systems where information about the system via the study of emission cannot be obtained. We note that for a proper interpretation of photoconductivity data it is almost always necessary to

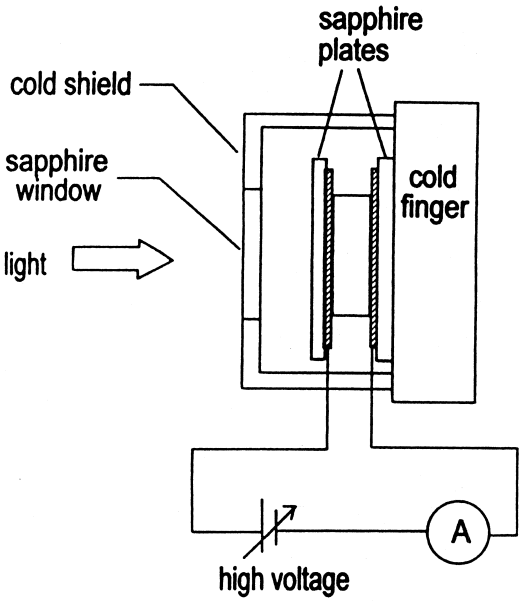

Fig. 2. Experimental setup for photoconductive studies on insulators.

complement photoconductivity spectra by standard absorption and photoexcitation techniques. For photoconductivity measurements the samples are mounted onto the cold finger of a temperature variable liquid nitrogen cryostat; pressed between two nickel meshes serving as transparent electrodes (Fig. 2). Nickel is used as an electrode material because of the high work function of this metal, and spurious currents due to the photoelectric effect do not occur at wavelengths longer than 250 nm. Other electrode materials, such as Au, Cu and stainless steel produce results similar to those obtained with Ni electrodes. The electrodes are electrically insulated from the copper mount by sapphire plates. To ensure proper cooling of the sample, the sample mount is equipped with a cold shield, resulting in a base temperature of 79 K. A temperature controller allows temperature dependent measurement between 79 K and room temperature. Photocurrents are excited by a 300 W Xe arc lamp spectrally filtered by an f/2 double grating monochromator (McPherson). A double monochromator is necessary to suppress straylight. The photocurrent is measured with a Keithley 6517 electrometer. To utilize the high sensitivity of the electrometer, additional features of the setup include electric shielding and high mechanical stability, resulting in a detectable photocurrent of less than 10^{-15} A. Typically, a field of up to 10,000 V/cm is applied across the sample which results in stationary photocurrents on the order of 10^{-15} A to 10^{-12} A.

4. Luminescence efficiency of cerium doped oxides

While the study of phosphor and scintillator materials generally focuses on systems with a high quantum efficiency, a thorough understanding of why certain systems show a very low quantum yield will lead to a better understanding of luminescent materials in general. As an example of the importance of the location of the impurity energy levels with respect to the host bands, we present results on Lu_2O_3: Ce^{3+} [13]. This material is characterized by a complete quenching of the Ce^{3+} 5d–4f luminescence. With the help of extensive absorption, photoexcitation and photoconductivity studies on single crystals, we could experimentally verify that the quenching mechanism is determined by the location of the Ce^{3+} 5d levels with respect to the host conduction band. Fig. 3 shows the absorption spectrum of Lu_2O_3:Ce^{3+} (solid line). It is characterized by a dominant absorption around 400 nm. At wavelengths shorter than 250 nm we observe the onset of strong band to band absorption (the band gap of Lu_2O_3 is about 6.5 eV). The absorption band cannot be found in undoped samples (Fig. 3, dashed line), and are also absent in doped samples annealed in air, which contain mainly Ce^{4+} ions (Fig. 3, dotted line) and exhibit an onset of a strong absorption band around 375 nm, which is due to an acceptor-like electron transfer from the host valence band to the Ce^{4+} ion. According to the Born–Haber cycle [6,7], the sum of the acceptor-like and donor-like thresholds must equal the energy gap between the host valence and conduction band (see Fig. 1). Using the values of the acceptor-like threshold of 375 nm (3.3 eV) found for Ce^{4+} and the onset of the predominant Ce^{3+} absorption band around 450 nm (2.8 eV) from our data, combined with the host band gap of 6.5 eV, the Born–Haber cycle predicts that the 400 nm band reflects a transition that can promote the 4f electron close to the host conduction band. The absence of any detectable characteristic cerium emission in Lu_2O_3:Ce^{3+} and the Born–Haber cycle analysis of the optical spectra leads to the conclusion that the strong absorption around 400 nm, although clearly related to the Ce^{3+} ion, cannot be a simple 4f– 5d transition. Instead, the strong absorption band reflects a donor-like electron exchange processes. This is confirmed by the photoconductivity spectrum of Lu_2O_3:Ce^{3+} presented in Fig. 4. The observed photocurrent is stationary, i.e. a steady current without a build-up of polarization in the sample. There is a striking similarity between the photo-induced current and the absorption: both are characterized by a strong band around 400 nm. The 400 nm photoconductivity band is not observed for undoped samples, whereas for doped samples annealed in air it is nearly 2 orders of magnitude smaller, thus the photoconductivity signal is strongly correlated with the Ce^{3+} absorption. At low temperature, the photoconductivity rises around 480 nm, thus we conclude that the Ce^{3+} groundstate lies 2.6 eV below the host conduction band. The Born–Haber cycle, using the band gap and the charge transfer energy E_A predicts a value of 3.2 eV. The difference of 0.6 eV is within the range of typical deviations between Born–Haber cycle predictions and experiments. In our case the deviation might be due to uncertainties in the band-gap value. Thus, the lack of

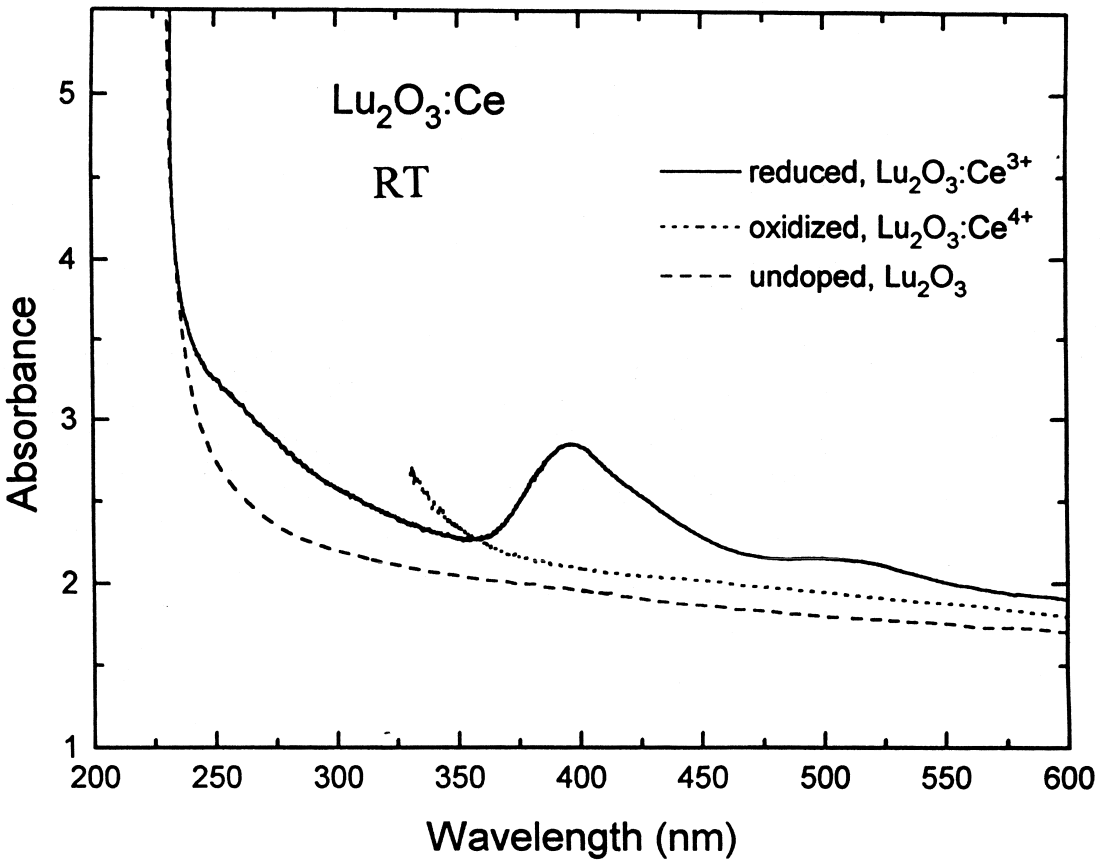

Fig. 3. Room temperature absorption spectra undoped and cerium doped Lu_2O_3.

luminescence, combined with the observed photoconductivity spectra and the Born–Haber analysis of both Ce^{3+} and Ce^{4+} absorption spectra is consistent with a 5d level of the trivalent cerium ion lying within the conduction band. An excited electron relaxes to the bottom of the conduction band, which is below the lowest Ce^{3+}-5d level. Thus, the electron does not return to this level, but relaxes in a non-radiative relaxation process to the Ce^{3+} ground state, causing the quenching of the luminescence.

We note that in other Ce^{3+} doped materials, like $Lu_2(SiO_4)O$ and $Y_2(SiO_4)O$ similar investigations have shown that in these very efficient scintillators the lowest 5d level lies below the host conduction band, again demonstrating the importance of the relative position of impurity energy levels with respect to the host bands [3].

5. Photoconductivity studies on micro-crystalline phosphor materials

While the above presented results were obtained on single crystals, a large number of interesting system are available readily, and some exclusively, in powder form. This is particularly true for phosphor material, where the particle size is one of many parameters used to fine-tune the phosphor performance. For photoconductivity studies the geometry shown in Fig. 2 cannot be used, even if the material is pressed into pellets, due to the strong light scattering of the powder. The scattering would lead to non-illuminated regions in the back of the sample and, in turn, to a suppression of the photocurrent. We use a configuration where nickel electrodes are evaporated on a thick sapphire window, leaving a 1 mm wide gap between the electrodes (Fig. 5). The window is placed in a sample holder which is designed to act as a press. The phosphor material is loaded on top of the sapphire plate and subsequently presses directly onto the electrodes using a second sapphire window. It must be expected that the conductivity measurements will be influenced by surface effects. To study the surface effect and to test the applicability of photoconductivity studies to microcrystalline powder, we compared the photoconductivity spectrum of CaS:Eu powder, a commercial phosphor, to that of a CaS:Eu single crystal. This system is known to exhibit temperature quenching of the Eu^{2+} d–f luminescence, indicating that the $4f^6 5d$ emitting level of Eu^{2+} is located rather close to the conduction band bottom (Fig. 6). Assuming that the quenching results from thermal ionization of the Eu^{2+} $4f^6 5d$ state, the energy difference between the $4f^6 5d$ excited state and the conduction band bottom has been assigned a value of $\Delta E = 0.13$ eV [14]. While this value is certainly important as an effective and practically

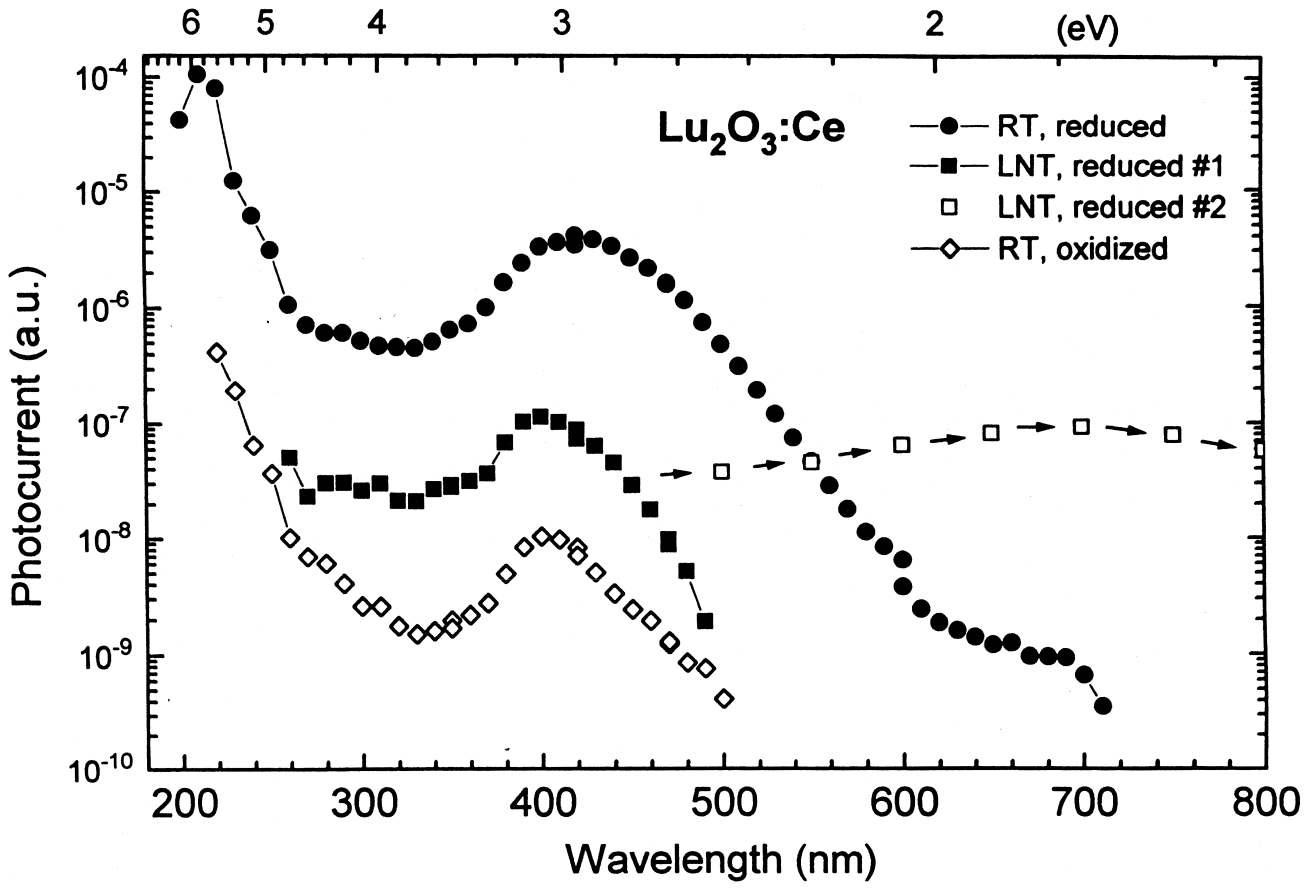

Fig. 4. Photocondcutivity spectra of $Lu_2O_3:Ce^{3+}$ at different temperatures. Data points marked by squares were obtained by scanning the excitation source from short to long wavelength, demonstrating the presence of shallow traps which were filled during short wavelength illumination.

important energy threshold, it might not represent the actual difference between the $4f^6 5d$ level and the conduction band. Fig. 7 shows the photoconductivity spectrum of a $CaS:Eu^{2+}$ single crystal for different temperatures. At room temperature, the photocurrent rises at about 790 nm, and increases by about 6 orders of magnitude to reach a plateau at about 600 nm. At subsequent lower temperatures, this threshold shifts to shorter wavelengths, and at 80 K a spectrum has evolved containing two thresholds. The threshold at 650 nm we attribute to electron tunneling from the excited $4f^6 5d$ Eu^{2+} level to a neighboring Eu^{3+} ion, since the current follows the Eu^{2+} absorption spectrum in the region of the main Eu^{2+} zero phonon line and shorter wavelengths [15]. In addition, the presence of Eu^{3+} ions has been confirmed by the detection of low-lying f–f transitions in our sample (this is an example for our statement that photoconductivity is a powerful spectroscopic tool when complemented by other optical tech-

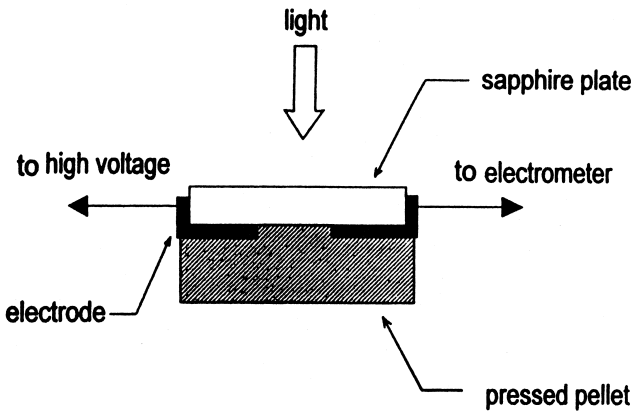

Fig. 5. Sample mount for conductivity measurements on microcrystalline powder.

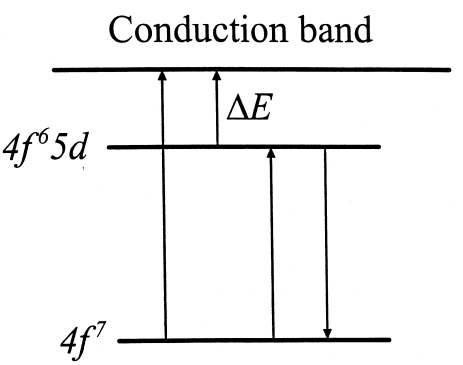

Fig. 6. Energy levels of Eu^{2+} in CaS.

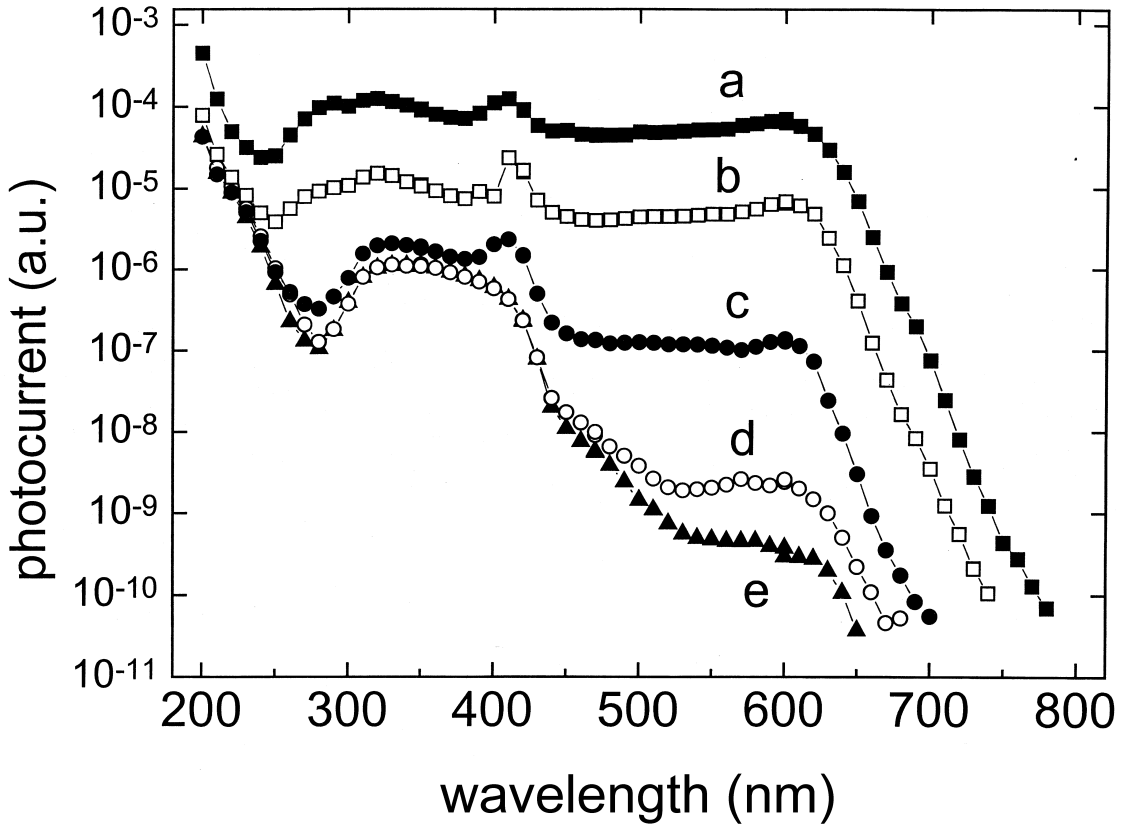

Fig. 7. Photoconductivity spectra of single crystal CaS:0.1%Eu. a: 300 K; b: 250 K; c: 200 K; d: 150 K; e: 80 K.

niques). We interpret the rise at 540 nm, the most important feature of the spectrum, as a direct excitation of an Eu^{2+} ion to the conduction band. From this we can directly evaluate ΔE:

$$\Delta E = h\nu - h\nu_{ZPL} = 0.3 \text{ eV}$$

where ν_{ZPL} is the frequency of the Eu^{2+} zero phonon line. This value has been confirmed by measuring the thermally activated current as a function of temperature under optical excitation. Returning to the problem of conductivity measurements on powders, Fig. 8 shows the corresponding photoconductivity spectra obtained on CaS:Eu^{2+} powder. We find spectra very similar to those obtained on the crystalline samples: two thresholds are clearly visible at low temperatures, and again we find the broad plateau at room temperatures, starting around 600 nm. The main difference is a signal beyond 700 nm at room temperature that we attribute to shallow traps, possibly at the surface of the powder. These results demonstrate the feasibility of photoconductivity measurements on microcrystalline phosphor materials.

6. Laser cooling of solids

There are a variety of phenomena that are due to ionization via excited state absorption, thus the location of the impurity levels relative to the host conduction band is important. An example is the reduction of the gain of solid state laser materials by promoting electrons from the emitting levels to the conduction band. An application where excited state absorption can not be tolerated is laser cooling of solids. Laser cooling of a solid may occur when the average energy of the photons emitted by the solid is larger than the energy of the absorbed photons. The energy difference is provided by phonons, thus leading to a net cooling of the solid. The principle of the laser cooling process is shown in Fig. 9. An important additional requirement is that non-radiative relaxation processes can be neglected. Mungan and Gosnell have published a detailed review about the history and recent results on laser cooling [16]. First successful cooling of a solid by 16 K was achieved in Yb^{3+} doped ZBLANP by a Los Alamos group [17]. This glassy system was chosen for its virtual lack of non-radiative relaxation processes and its high purity, which suppresses absorption processes due to unwanted impurities. After the first success, Yb^{3+} doped ZBLANP has been cooled by 21 K [18], but no laser cooling of other systems have been reported. This might be partly due to unwanted impurities in the investigated systems, however, we have found that excited state absorption is a likely process that could prohibit laser cooling. To our knowledge, this process has been overlooked in the context of laser cooling of Yb^{3+} doped solids. We have

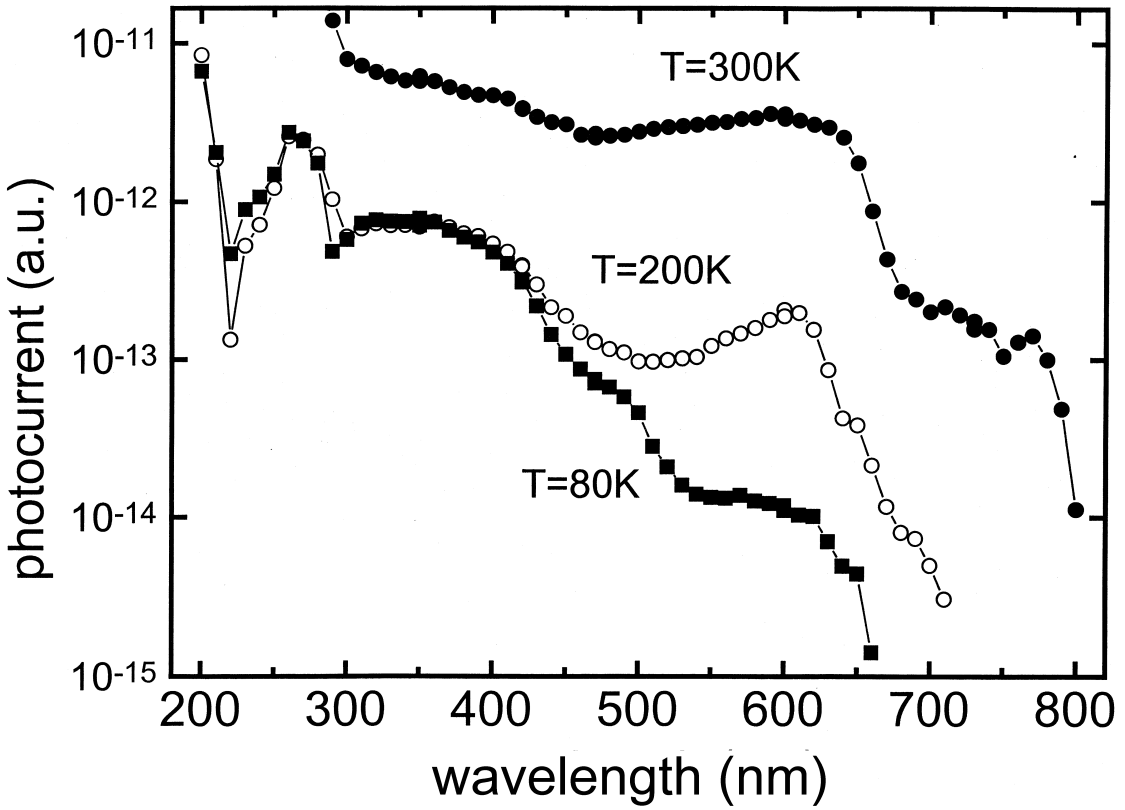

Fig. 8. Photoconductivity spectra for CaS:0.7%Eu powder.

investigated Yb^{3+} doped α-Al_2O_3 (sapphire). It is generally difficult to introduce rare earth ions into sapphire using conventional crystal growth techniques, however, rare earth doped α-Al_2O_3 can be obtained in a sol–gel process [19]. We also succeeded to grow Yb^{3+} doped sapphire via laser heated pedestal growth technique [20]. To confirm that Yb^{3+} occupies a site of the α-Al_2O_3 structure, we compared the emission and absorption spectra of our samples with that of other Yb^{3+} containing crystal structures. We have performed photoconductivity measurements on this system to locate the Yb^{3+} groundstate with respect to the host conduction band. Fig. 10 shows the obtained photocurrent as a function of excitation wavelength. The current rises around 640 nm (1.9 eV), which we interpret as the threshold for a donor-like electron transfer process. To have an independent confirmation for this assignment, we performed photoexcitation measurements at a few argon ion laser and HeNe laser wavelengths, i.e. we monitored the Yb^{3+} $^2F_{5/2}$ to $^2F_{7/2}$ emission under laser excitation. The result is plotted as solid circles in Fig. 10. We find a threshold for the excitation of the Yb^{3+} emission which coincides with the photoconductivity signal. Excitation at shorter wavelengths leads to a stronger photoexcitation signal, following the shape of the photoconductivity curve. The photoexcitation signal reflects the promotion of an Yb^{3+} electron to the conduction band. This electron is subsequently trapped by the Yb^{4+} ion, resulting in an excited Yb^{3+} ion which relaxes to the ground state under emission of characteristic Yb^{3+} emission. From our results we obtain directly the location of the Yb^{3+} energy levels with respect to the conduction band, the result is shown in

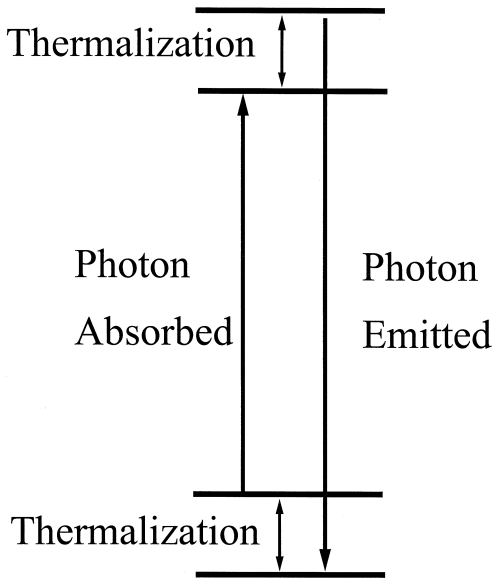

Fig. 9. Energy-level diagram for an impurity ion in a solid host. The arrows indicate pump and relaxation processes leading to laser cooling of the system.

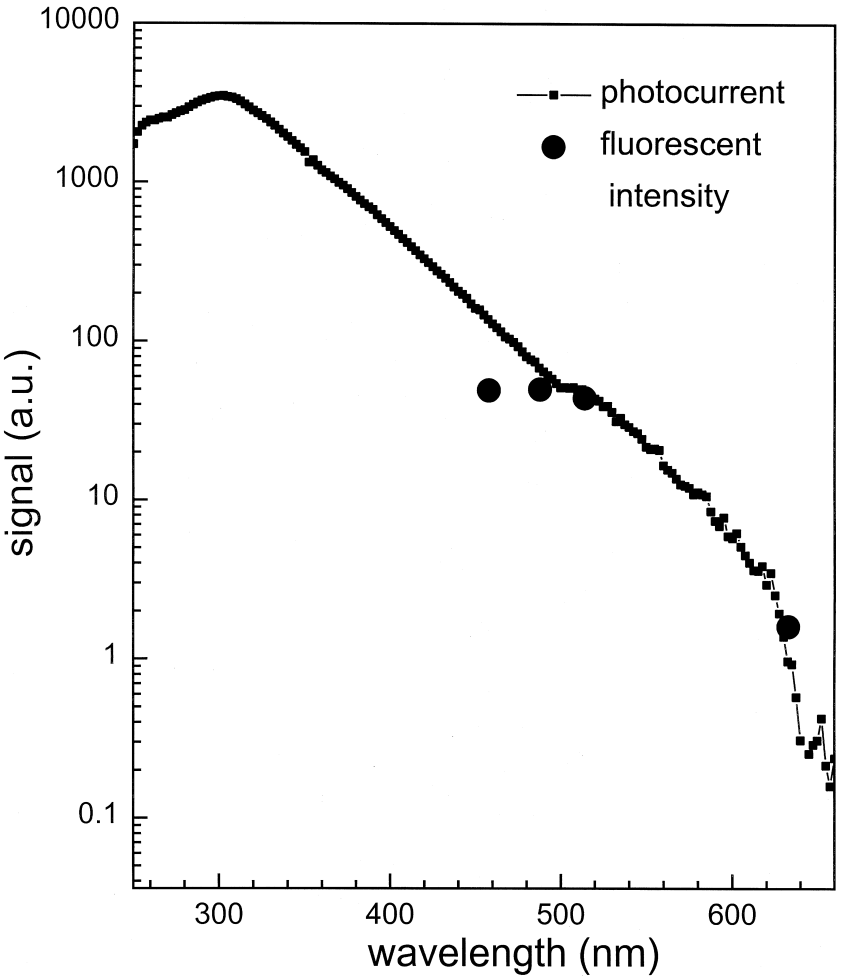

Fig. 10. Photoconductivity of Al_2O_3:Yb^{3+} as a function of excitation wavelength (squares). The circles represent the fluorescence intensity of the sample under optical excitation, normalized to the laser intensity.

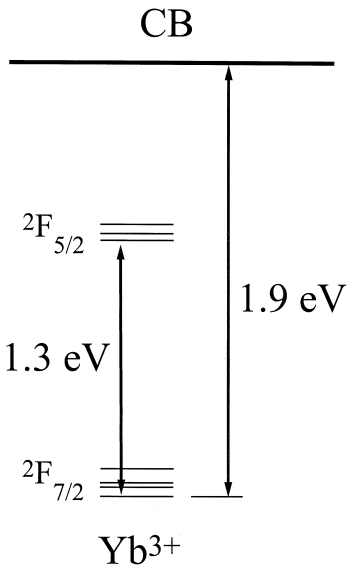

Fig. 11. Position of the Yb^{3+} energy levels with respect to the sapphire conduction band.

Fig. 11. The intra-ion f–f transition occurs around 1.3 eV, which is about the same for Yb^{3+} in glasses and crystals. For sapphire, the excited state lies only 0.6 eV below the conduction band. Thus, the Yb^{3+} groundstate lies relatively close to the host conduction band (compared to the host band gap of about 10 eV [21]) and pumping of the Yb^{3+} f–f transition will be accompanied by excited state absorption, followed by non-radiative relaxation processes, prohibiting laser cooling of this system. We are in the process of studying a number of Yb^{3+} doped materials in order to establish a list of promising ytterbium doped materials for laser cooling.

7. Conclusions

We have presented a small number of examples that demonstrate that electron processes play an important role in the luminescence efficiency of doped insulators. Further, we have used a donor/acceptor-like treatment of the impurity-host interaction to fully describe the optical

properties of rare earth doped materials. Experimentally, we have shown that photoconductivity, combined with other optical techniques, is a powerful technique to determine the location of the impurity energy levels with respect to the host bands. While this paper is mainly concerned with the experimental aspect of electron transfer processes, we would like to mention that fairly recently the energy levels of impurities in insulators have become the focus of theoretical investigations. That this field has been neglected for a long time is partly due to the large computational effort necessary for some of the new approaches used. While generally the obtained results deviate for even undoped systems from experimental results, large progress has been made in recent years, and we expect a growing number of collaborative efforts between theory and experimental groups to provide answers for the fundamental questions about the origin of the exact position of impurity levels in doped insulating materials.

Acknowledgements

The authors thank D.S. McClure, G.F. Imbusch. A.A. Kaplyanskii, C.E. Mungan, and W.M. Yen for many stimulating discussions.

References

[1] B. Henderson, G.F. Imbusch, Optical Spectroscopy of Inorganic Solids, Clarenson Press, Oxford, 1989.
[2] W.C. Wong, D.S. McClure, S.A. Basun, M.R. Kokta, Phys. Rev. B51 (1995) 5682.
[3] M. Raukas, S.A. Basun, W. van Schaik, W.M. Yen, U. Happek, Appl. Phys. Lett. 69 (1996) 3300.
[4] G. Blasse, B.C. Grabmeier, Luminescent Materials, Springer, Berlin, 1994.
[5] R.M. Macfarlane, R.M. Shelby, in: W.E. Moerner (Ed.), Persistent Spectral Holeburning; Science and Applications, Springer Verlag, Berlin, 1988, p. 127.
[6] M. Born, Verh. Dtsch. Phys. Ges. 21 (1919) 679.
[7] F. Haber, Verh. Dtsch. Phys. Ges. 21 (1919) 750.
[8] C. Kunz (Ed.), Synchrotron Radiation; Techniques and Applications, Topics in Current Physics, Vol. 10, Springer-Verlag, Berlin, 1979.
[9] R.H. Bube, Photoconductivity of Solids, John Wiley & Sons, New York, 1960.
[10] A. Rose, Concepts in Photoconductivity and Allied Problems, Interscience Publishers, New York, 1963.
[11] D.S. McClure, C. Pedrini, Phys. Rev. B 32 (1985) 8465.
[12] C. Pedrini, F. Rogemond, D.S. McClure, J. Appl. Phys 59 (1986).
[13] W.M. Yen, M. Raukas, S.A. Basun, W. van Schaik, U Happek, J. Lumin. 69 (1996) 287.
[14] M. Ando, Y.A. Ono, J. Cryst. Growth 117 (1992) 969.
[15] S.A. Basun et al., Phys. Rev. B56 (1997) 12992.
[16] C.E. Mungan, T.R. Gosnell, in: B. Bederson, H. Walter (Eds.), Laser Cooling of Solids, in Advances in Atomic, Molecular, and Optical Physics, Academic Press, San Diego, 1999, p. 161.
[17] C.E. Mungan et al., Phys. Rev. Lett. 78 (1997) 1030.
[18] X. Luo, M.D. Eisaman, T.R. Gosnell, Opt. Lett. 23 (1998) 639.
[19] A.A. Kaplyanskii et al., Phys. Solid State 40 (1998) 1310.
[20] W.M. Yen, J. Alloys Comp. 193 (1993) 175.
[21] E.T. Arakawa, M.W. Williams, J. Phys. Chem. Solids 29 (1968) 735.